Available online at www.sciencedirect.com
SCIENCE DIRECT®
Physics and Chemistry of the Earth 31 (2006) 164–171
PHYSICS and CHEMISTRY of the EARTH
www.elsevier.com/locate/pce

On the origin of stable IR anomalies detected by satellites above seismo-active regions

V.V. Surkov [a,*], O.A. Pokhotelov [b], M. Parrot [c], M. Hayakawa [d]

[a] Moscow State Engineering Physics Institute, 115409 Moscow, 31 Kashirskaya Road, Russia
[b] Institute of Physics of the Earth, 123995 Moscow, 10 Bolshaya Gruzinskaya Street, Russia
[c] Laboratoire de Physique et Chimie de l'Environment, Centre National de la Recherche Scientifique, Orleans, France
[d] The University of Electro-Communications, 182-8585 Chofu, Tokyo, Japan

Accepted 6 February 2006
Available online 19 May 2006

Abstract

A number of experimental evidences have recently been obtained for existence of stable anomalies of infra-red outgoing Earth radiation in seismo-active regions, basically by using NOAA-series satellite data. A theoretical model for temperature enhancement of the ground surface layer in the vicinity of fault system of the Earth's crust is developed. It is assumed that a tectonic stress in this area results in a water squeezing-out from the higher depths towards the Earth's surface. A convection mechanism of rock warming by groundwater upward filtrating is considered as a possible reason for stable temperature anomalies arising near the fault interception. According to this model the fluid filtrates upwards from the higher depth to the Earth's surface to provide an increase in the ground temperature similar to that found in observations.

Keywords: Infrared radiation; Groundwater filtration; Convection heat transfer; Rock heat conductivity; Rock permeability

1. Introduction

A special credit has been paid in the last decade to monitoring of the seismo-active regions from space in visible and infrared (IR) ranges (e.g., Qiang et al., 1991, 1992; Qiang and Dian, 1992; Qiang et al., 1999; Salman et al., 1992; Tronin, 1996, 1999, 2002; Tronin et al., 2002; Liu et al., 2000; Tramutoli et al., 2001; Carreno et al., 2001; Ouzounov and Freund, 2004). Due to high spatial resolution this method was considered as perspective for the analyses of lineaments, morphological structures and tectonic movements (Veber, 1984). An advanced space-borne equipment for remote sensing in the IR spectrum allows us to study the ground-surface temperature with a spatial resolution of 0.5–1 km and with a temperature resolution of 0.1–0.5 K (Wan and Li, 1997). The NOAA-series satellite survey has been used for detection of variations of the outgoing IR radiation. This technique may also provide a possibility to locate the major forthcoming earthquakes. On one hand, the minimal absorption of IR by the atmosphere corresponds to wavelengths of 3–5 μm and 8–13 μm. On the other hand, for the actual ground surface temperature that lies in the range of 273–373 K, the radiation peak corresponds to 7.7–10.5 μm. These two factors are in favour of using the IR monitoring in the range of 8–13 μm (known as a second transparency window) for the earthquake studies. As compared with the near-IR and visible ranges this part of the spectrum is due to the surface ground temperature (Tronin, 1999). The nighttime conditions are the most favorable for the IR monitoring of the ground-surface temperature since there are no solar heating. Thus the effects due to surface and underground sources can be dominant. The seismo-active regions of Central Asia including Tien-Shan, Kizilkum and Karakum

* Corresponding author. Tel.: +7 95 3239835; fax: +7 95 3007516.
E-mail address: surkov@redline.ru (V.V. Surkov).

1474-7065/$ - see front matter © 2006 Elsevier Ltd. All rights reserved.
doi:10.1016/j.pce.2006.02.020

deserts and South Kazakhstan have been extensively studied in the past (Gorny et al., 1988; Tronin, 1999). The analysis of the nighttime IR radiation provided by these studies revealed the presence of anomalies of the outgoing Earth's radiation flux associated with large structures and fault systems of the Earth's crust. The satellite measurements carried out during nighttime conditions have pointed out on an increase in the average ground temperature of several Kelvin at the foot of Kopetdag in Central Asia. The anomaly area was 25–30 km wide and about 500 km in length. Another type of anomaly of about 50 km wide and 300 km long was found at the foot of the Karatau Range that roughly coincides spatially with the Karatau Fault. These stable IR anomalies have been also observed at some other faults, though the extent and average intensity of anomalies can vary in time. A close correlation between such variations and seismic activity prior to the Gazli earthquakes of 1976 and 1984 ($M > 7.0$) was mentioned by Gorny et al. (1988). These strong earthquakes appeared close to interception of the Tamdy-Torkaus and Karatau faults. An extended area of non-stable anomaly was observed in the Talasso-Fergana fault zone in Central Asia prior to crustal earthquakes with magnitudes greater than 4.3. Similar studies were also carried out in China (Ma and Gao, 1991; Qiang et al., 1991, 1999), European Union (Tramutoli et al., 2001) and Japan (Hayakawa et al., 2001). Based on ground sensor measurements, soil temperature anomalies of 2.5 K were observed in the preparation zone of the 1976 Tangshan earthquake (China), which had a magnitude more than 7.0 (Wang and Zhu, 1984).

A novel method of data analysis related to the remote detection of the thermal anomalies was proposed by Tramutoli et al. (2001). In this paper the data collected during several years were used to evaluate the space–time average temperature. The local deviation of the brightness temperature normalized to standard deviation was considered to be an indicator of the ground temperature anomaly. This procedure promotes the reduction of the climatological and other effects. The capability of the refined noise-removal approach has been demonstrated for the case of the Irpina-Basilicata earthquake of November 23, 1980 ($M_s = 6.9$).

The origin of such stable and non-stationary IR anomalies is not entirely clear whereas some effects (hydro-geological or greenhouse effects) are considered to be a probable candidate for the formation of the anomaly (Tronin, 1999; Hayakawa et al., 2001). Solar radiation affects the surface temperature and the geothermal and meteorological fluxes. The geothermal flux consists of two components: conductive and convective. For the Central Asia the first one, which was estimated as 40–100 mW/m^2, is smaller than the flux due to the solar radiation by several orders of magnitude. While the convective heat flux connected with the underground fluid and gas movement can exceed several tenths of W/m^2. Some geological structures, e.g., of rift-origin, can also produce high geothermal fluxes.

We cannot come close to exploring all these problems in any detail. The mechanisms of the non-stationary IR anomalies are outside the scope of the present paper and can be discussed in a separate publication. The main goal of our paper is to study the stable IR anomaly and the convective geothermal transfer as a possible cause of the ground surface temperature enhancement. The paper is organized in the following fashion: Section 2 is devoted to the theory of formation of permanent surface temperature anomalies occasionally observed near the fault zone. Our discussion and conclusions are found in Section 3.

2. Convective heat transfer caused by groundwater

It is of common knowledge that rocks contain fluid-filled pores and cracks at high depths. The tectonic processes and the deformations in the vicinity of the fault zone result in both fresh crack formation and squeezing-out of water from higher depths towards the ground surface. The crack formation at higher depths might be accompanied by the competitive processes of the crack healing (Scholz, 1990) and thus the permeability of the rocks could vary in time and in space. One should emphasize that a stable system of interacting cracks or pore channels is not required to produce a gradual fluid leakage.

Let us assume that the deformation and fracture of the rocks reinforce this long-term process that develops for geological time. So the fluid is capable to filtrate upwards through the network of channels distributed in the upper layers of the Earth's crust which have the thickness of about several kilometers. The temperature in the lower layers is higher than in the upper layers. The same is true for the groundwater, and due to that the water moving upwards can heat the upper-lying ground layers. In what follows, this convection mechanism of the rock heating by the groundwater is subjected to theoretical analyses in greater detail to provide an answer to the question whether this mechanism can explain the above-mentioned surface ground temperature anomalies in seismo-active regions.

To proceed analytically, it is necessary at this point to construct a suitably idealized model of the medium, which is assumed to contain a stable system of interconnected channels. The temperature is assumed to be growing linearly with depth z in a way that the modulus of temperature gradient, α, remains to be equal to $\approx$0.01–0.02 K/m. The heat conductivity β_g, the specific heat capacity c_g and the mass density of the ground ρ_g are assumed to be constant values. Let us first consider the fraction AB of one of the channels (Fig. 1a) that can be considered approximately as a linear channel. We introduce the local Cartesian system of coordinates (x_1, y_1, z_1), with the z_1-axis pointing downward along the axis of our channel. This axis forms the angle θ with the vertical axis z. According to the known Darcy's law, the velocity of fluid filtration is

$$\mathbf{v} = -\frac{k}{\eta}\nabla P, \tag{1}$$

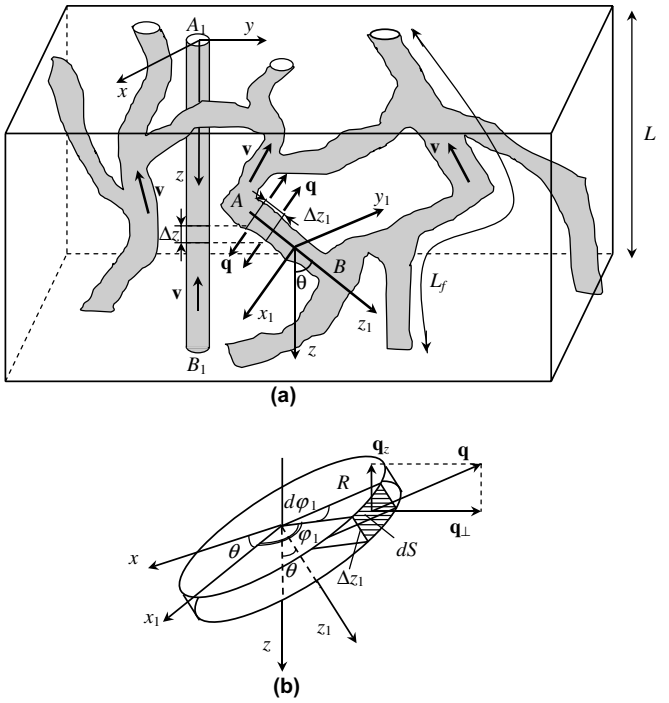

Fig. 1. Schematic plot of the convection mechanism model for rock heating by underground filtrating water. Here **v** denotes the velocity of a fluid, filtrating along the channels and **q** stands for the heat flux density. (a) General scenario. (b) A small fraction of the channel.

where k is the rock permeability, η is the fluid viscosity and P denotes the fluid pore pressure.

The fluid velocity may vary with depth due to the change in the rock permeability, porosity, channel tortuosity, rock deformation and etc. According to Mizutani et al. (1976) and Scholz (1990) the typical rock parameters are as follows $|\nabla P| = 10^2$–10^4 Pa/m and $k = 10^{-12}$–10^{-14} m^{-2}. If the infiltration is a predominant mechanism for the interstitial water motion, the strata pressure gradient cannot be greater than the hydrostatic pressure gradient, i.e., 10^4 Pa/m. If the groundwater migration results from the water squeezing-out under the influence of tectonic stress, the pressure gradient can achieve geostatic pressure gradient, i.e., $\sim 2 \times 10^4$ Pa/m, and even exceed this level (Barsukov, 1990). Nevertheless, we have not reliable information on the pressure gradient in the deep crust. Substituting $k = 10^{-12}$ m^2, $|\nabla P| = 10^2$ Pa/m and $\eta = 10^{-4}$ Pa s into Eq. (1), gives the rough estimate $v = 10^{-6}$ m/s.

Despite small value of the filtration velocity, the convective heat transport of the moving fluid seems to be more effective than the conductive mechanism. Before comparing these two mechanisms in the fluid, we should note that the heat conduction is controlled by a diffusion coefficient $D_F = \beta_F/(c_F\rho_F)$, where β_F is the fluid thermal conductivity, and c_F and ρ_F are the specific heat capacity and mass density of the fluid, respectively. The conductive heat transfer obeys the diffusion law in a way that the heat front propagates as $r_f(t) \approx (D_F t)^{1/2}$, where r_f denotes its position at moment t. Using $t = 1$ year as typical time for this process,

Table 1
Typical parameters of abyssal (basalt and granite) and sedimentary (sandstone, loam, limestone and dolomite) rocks under atmospheric pressure (Babichev et al., 1991; Clark, 1966, 1969)

Substance	$\rho \times 10^3$, kg/m^3	c, kJ/kg K	β, W/(m K)	β_a, W/(m K)
Water	1	2–5 ($T = 300$–600 K)	0.42–0.56	0.49
Basalt	2.6–3.3	0.85–1.49 ($T = 273$–1473 K)	0.44–3.5	1.3
Granite	2.3–2.8	0.65–1.30 ($T = 273$–1073 K)	1.1–3.9	2.4
Sandstone	1.9–2.7	–	0.24–4.4	1.8
Loam	1.6–2.9	0.8 ($T = 300$ K)	0.12–3.1	1.6
Limestone	2.7–2.8	–	0.64–4.4	2.3
Dolomite	2.84	0.93 ($T = 293$–372 K)	1.6–6.5	3.2

Here ρ is the rock mass density, c is the specific heat capacity, β is the thermal conductivity and β_a denotes the average value of β.

$\beta_F = 0.56$ W/(m K), $\rho_F = 10^3$ kg/m^3 and $c_F = 2.5$ kJ/kg K (Table 1) we obtain $r_f \approx 3$ m. Taking $v = 10^{-6}$ m/s one can find that during this time the fluid may pass a distance $vt \approx 30$ m which is much greater than that due to thermal conductivity. This means that convection mechanism of heat transfer in the fluid is more preferable and should be considered as dominant for typical time intervals.

Since we are interested only in the rough estimations it is reasonable to assume that the fluid velocity in the given fraction of the channel is nearly constant and equals to its mean value. We propose also that the neighboring channels do not influence the heat transfer in the region surrounding the selected channel. Such an assumption is justified by the fact that the heat conduction in rocks is quite slow process. The quantitative estimations will be presented below.

According to above estimate, we will neglect the heat transfer due to thermal fluid conductivity. Assuming for the moment that the given fraction of the channel has approximately cylindrical form with the radius R, then the gradient of the convective heat flux in a channel has only longitudinal z-component, that can be written as

$$d_z\dot{Q} = \pi R^2 v \rho_F c_F d_z T. \tag{2}$$

Here the dot denotes the derivative over time, v is the velocity of a fluid filtration, T is the fluid temperature and $d_z \equiv \mathrm{d}/\mathrm{d}z_1$ denotes derivative over z_1. In the simplified model under consideration, the fluid parameters depend solely on the temperature. This dependence is especially essential at a higher depth where the state of a fluid is close to critical state. In our case **v**, ρ_F and c_F in Eq. (2) can be considered as constant values. Thus, only the temperature varies with depth, i.e., $T = T(z)$.

To study the thermal balance at the channel surface we first consider a narrow cylindrical layer of a channel bounded by the z_1 and $z_1 + \Delta z_1$ cuts (Fig. 1a and b). The change in the convective heat flux through the channel cross section equals to the heat flux flowing through the channel side surface. Taking into account that the vector of heat flux density, **q** (the heat flux through the unit surface per unit time) is directed outwards we obtain

$$2\pi R\int_{z_1}^{z_1+\Delta z_1} q\,\mathrm{d}z_1 = \dot{Q}(z_1+\Delta z_1) - \dot{Q}(z_1). \tag{3}$$

Here it is assumed that the vector **q** is perpendicular to the channel surface while the absolute value of **q** does not depend on the azimuthal angle φ_1 (see Fig. 1b). According to Eq. (3), the radial component of the heat flux defined on the channel surface, q, is

$$q = \frac{1}{2\pi R} d_z \dot{Q}. \tag{4}$$

Substituting Eq. (2) in Eq. (4) we obtain

$$q = \frac{1}{2} v \rho_F c_F R d_z T. \tag{5}$$

Since the temperatures of the fluid and surrounding rocks are only slightly different from each other, we can substitute $d_z T = \alpha$ into Eq. (5) for the case of vertical channel and $d_z T = \alpha\cos\theta$ for the case of inclined channel. Thus we get

$$q(R, z_1) = \frac{1}{2}\rho_F v c_F R \alpha \cos\theta. \tag{6}$$

In a first approximation we now replace the inclined channel treated here by an effective vertical fraction with the length $\Delta z = \Delta z_1 \cos\theta$ under the requirement that the same heat flux flows through the sides of this effective channel (Fig. 1a and b). The total heat flux ΔQ, flowing through the sides of the inclined channel, is $\Delta Q = 2\pi R \Delta z_1 q$. Then the mean heat flux density, flowing through the sides of the inclined channel, is $\langle q\rangle = \Delta Q/(2\pi R\Delta z) = q/\cos\theta$, where q is given by Eq. (6). Since $\langle q\rangle$ is independent of θ we can thus replace the real tortuous channel by the effective vertical channel A_1B_1 (Fig. 1a), where on the side surfaces the mean flux density is equal to $\langle q\rangle$. This implies that we now consider an idealized pore space geometry that ignores the channel curvature. Assuming continuity condition for a heat flux at the boundary of the channel and using cylindrical coordinates (r, z) at $r = R$, yields

$$\beta_g \partial_r T(R, z) = \frac{1}{2} R v \rho_F c_F \alpha, \tag{7}$$

where β_g stands for the ground thermal conductivity.

In fact, the boundary condition (7) we have thus far obtained takes into account only the heat flowing through the channel sides in horizontal directions. Below we will show that Eq. (7) gives a reasonable approximation to real boundary condition at the channel sides. In the case of the oblique channel the heat flows through the channel sides not only horizontally but also upward and downward. In order to estimate the corrections to Eq. (7) that can arise owing to this fact, we consider an elementary heat flux, $\mathrm{d}Q = q\,\mathrm{d}S$, flowing through the channel side $\mathrm{d}S = R\mathrm{d}\varphi_1\Delta z_1$, that is shown in Fig. 1b with shaded area. This flux can be split into two parts, $\mathrm{d}Q = q_z \mathrm{d}S_z + q_\perp \mathrm{d}S_\perp$ the first one can be associated with the heat flux pointed upward and downward, and the second is the "horizontal" flux. The components, $\mathbf{q}_z$ and $\mathbf{q}_\perp$, of the vector **q** and the reference frames used in this study are shown in Fig. 1b. Here x, z-plane intersects the channel cross-section along the x_1-axis. Using Euler angles θ and φ_1 we obtain that $q_z \mathrm{d}S_z = q\cos^2\varphi_1 \sin^2\theta\,\mathrm{d}S$ and $q_\perp \mathrm{d}S_\perp = q(\cos^2\varphi_1\cos^2\theta + \sin^2\varphi_1)\mathrm{d}S$. Integrating these expressions over φ_1 gives the "vertical" and "horizontal" fluxes, $\Delta Q_z = \pi q R \Delta z_1 \sin^2\theta$ and $\Delta Q_\perp = \pi q R \Delta z_1(1+\cos^2\theta)$. One half of the flux ΔQ_z points downwards and thus should be subtracted from the total heat flux, which can be associated with the effective vertical channel A_1B_1. Therefore, the effective net flux can be estimated as $\Delta Q_{\mathrm{eff}} = 2\pi q R \Delta z_1 - \Delta Q_z/2$.

Actually the angle θ that defines the orientation of the oblique channels is a random value. Thus, the flux ΔQ_{eff} should be averaged over random orientations of the channels that are localized in the horizontal layer with the thickness $\Delta z = \Delta z_1 \cos\theta$. Using Eq. (6) we obtain

$$\langle Q_{\mathrm{eff}}\rangle = \frac{1}{4}\pi R^2 \Delta z v \rho_F c_F \alpha(3 + \langle\cos^2\theta\rangle). \tag{8}$$

If the channel directions are uniformly distributed in space, the mean value of $\cos^2\theta$ is derivable from straightforward calculations, i.e., $\langle\cos^2\theta\rangle = 1/3$. Once the actual geometry of the pore space is considered, the mean value of $\cos^2\theta$ can be expressed through the channel tortuosity which is defined as $b = L_f/L$ (De Groot and Mazur, 1962; Pfannkuch, 1972), where the meaning of L_f and L is clear from Fig. 1a. Hence, we obtain that $\langle\cos^2\theta\rangle \approx b^{-2}$. The mean heat flux density flowing through the vertical channel sides can be defined as $\langle q_{\mathrm{eff}}\rangle = \langle\Delta Q_{\mathrm{eff}}\rangle/(2\pi R\Delta z)$. Then, with the help of Eq. (8), we get the boundary condition

$$\beta_g \partial_r T(R, z) = \frac{1}{8} v \rho_F c_F R \alpha\left(3 + \frac{1}{b^2}\right). \tag{9}$$

It should be noted that the right-hand sides of Eqs. (7) and (9) coincide with each other within the numerical factor $k_0 = 0.25(3 + b^{-2})$, where $0.75 < k_0 \leqslant 1$. This means that the channel tortuosity weakly affect the boundary condition (9).

3. Thermal balance of the Earth's surface

In what follows we study the conductive heat transfer in the rock surrounding the fluid-filled channels. As we shall see, due to smallness of the thermal conductivity, β_g, the heat spreading in the rock is rather slow. This allows us to consider first the heat propagation from a single channel, neglecting the corresponding influence of the neighboring channels. Now we proceed with consideration of the effective vertical channel A_1B_1. The equation of thermal conductivity in the outer region, $r > R$, reads

$$\partial_t T = D_g \nabla^2 T. \tag{10}$$

Here $\nabla^2 = \partial_r^2 + r^{-1}\partial_r + \partial_z^2$, (r, z) denote the cylindrical coordinates and the diffusion coefficient is given by $D_g = \beta_g/c_g\rho_g$. We suppose that the heat flux density at infinity $(z \to \infty)$ is constant and approximately equals to the geothermal flux density $q_g = \beta_g\alpha$. This results in

$$\partial_z T = \alpha, (z \to \infty, r > R). \quad (11)$$

Condition (11) is valid for a certain range of depths, e.g., for distances of several tens of kilometers up to the mantle-crust boundary.

Eqs. (10) and (11) should be supplemented by the proper boundary conditions for the ground surface that takes into account the heat exchange between ground and atmosphere. The heat balance consists of the geothermal flux, q_g, heat transfer due to radiation, the turbulent heat exchange and losses, q_{ev}, due to fluid evaporation (Tronin, 1999). Below we will focus on estimation of the underground heat flux caused by the heat transfer due to filtration of the pore fluid. As was shown above, this process is very slow. Thus, the fast/diurnal variations of the boundary conditions at the ground are of minor importance. Thereby we may use the averaged value of solar radiation flux, q_s, and the averaged air temperature, T_a, in the lower atmospheric layer, i.e., we can neglect the diurnal variations of these parameters. The solar energy absorbed by the ground equals to the $q_s(1 - A)$, where A denotes the surface albedo. Let q_e be the thermal flux emitted from the ground. Then the thermal balance of absorbed and radiated energies is $q_r = q_s(1 - A) - q_e$. Thus, the temperature balance condition is

$$-\beta_g \partial_z T = \gamma(T_a - T) + q_r - q_g + q_{ev} \quad (z = 0, \ r > R), \quad (12)$$

where the term $\gamma(T_a - T)$ defines the convective heat exchange between the ground and the atmosphere. The constant γ varies from day to night as $\gamma = (15\text{–}25)$ W/(m^2 K) (Gorny et al., 1993). The solution of Eq. (10) with boundary conditions (7), (11) and (12) is given in Appendix A. Eq. (A.18) determines the average temperature increase, δT, at the ground surface $z = 0$ due to the heat transfer produced by underground fluid. The averaging was carried out over the large surface, whose radius, R_0, is much greater than the characteristic radius of the channels, R. Expression (A.18) takes also into account the effect of a single channel filled with moving fluid. We note that the change in temperature δT in Eq. (A.18) is proportional to vR^2, i.e., to the value which defines the fluid volume flowing through the perpendicular channel cross-section per unit time.

Now let us assume that the channels are distributed over their dimensions according to some law characterized by the distribution function $f(R)$, normalized to the number of the channels per volume, i.e.,

$$\int_0^\infty f(R)\,\mathrm{d}R = N.$$

Then the mean porosity n can be defined as

$$n = \pi \int_0^\infty R^2 L_f(R) f(R)\,\mathrm{d}R \sim \pi L b \int_0^\infty R^2 f(R)\,\mathrm{d}R, \quad (13)$$

where b is the mean channel tortuosity.

We note that the distribution function $f(R)$ as well as the mean porosity n are dependent of the depth z. The fluid volume flowing to the Earth's surface per unit time is defined by the mean porosity and permeability of the channels at large depths. Thus, in our calculations one should account for the values of the mean porosity that is typical for the high depths. Then the mean increase in the ground surface temperature, contributed by all channels contained in the volume $\pi R_0^2 L$, is

$$\delta T(t) = \pi R_0^2 L \int_0^\infty \delta T_1(t, R) f(R)\,\mathrm{d}R, \quad (14)$$

where $\delta T_1(t, R)$ is the mean access in the ground temperature caused by one of the channels.

Substituting expression (A.18) for $\delta T_1(t, R)$ into Eq. (14) we get

$$\delta T(t) = 2\alpha v \rho_F c_F L k_0 \frac{(\pi D_g t)^{1/2}}{\gamma} h(s) \int_0^\infty R^2 f(R)\,\mathrm{d}R. \quad (15)$$

Here the auxiliary function $h(s)$ is introduced, given by

$$h(s) = 1 - \frac{\pi^{1/2}}{2s^{1/2}}\left[1 - \exp(s)\mathrm{erfc}\left(s^{1/2}\right)\right], \quad (16)$$

where $s = t\gamma^2/(c_g \rho_g)$, $\mathrm{erfc}(x) = 1 - \mathrm{erf}(x)$ and $\mathrm{erf}(x)$ is the standard error function (Abramowitz and Stegun, 1964).

Rearranging Eq. (15) by introducing mean porosity n (Eq. (13)), we find that the net effect of all the channels reads

$$\delta T(t) = \frac{2n\alpha v \rho_F c_F k_0}{\gamma b} \left(\frac{D_g t}{\pi}\right)^{1/2} h(s), \quad (17)$$

where $k_0 = 0.25(3 + b^{-2})$. Eq. (17) is valid for the case of infinite channels but, in fact, it can be applied for finite channels under condition that $D_g t \ll L^2$, where L is the characteristic channel length. This condition is not so burdensome on account of low thermal conductivity of the ground.

It should be noted that Eq. (17) defines the local increase in the ground surface temperature. The most probable regions for such an increase correspond to the vicinities of the fault interceptions where the rock porosity and permeability can be higher than that for the background. The triggering mechanism for such an increase in the rock fracturing, permeability and other changes, which results in the formation of interconnected underground channels, can be due to the tectonic processes in the far past. In other words, the life time of such an anomaly is of the order of geological time-scales. Let us answer the question when the source of the thermal energy should be turned on in order to reach the ground surface temperature increase of $\delta T \approx 1$ K at present time. Such a value of δT was observed by Tronin (1999) and Tramutoli et al. (2001). For that we choose the following average values: $\beta_g = 2$ W/(m K), $c_g = 1$ kJ/(kg K), $c_F = 2.5$ kJ/(kg K), $\rho_g = 2 \times 10^3$ kg/m^3, $\rho_F = 10^3$ kg/m^3 (the subscripts "g" and "F" refer to the ground and the fluid, cf. Table 1), $\gamma = 19$ W/(m^2 K), $v = 10^{-6}$ m/s, $n = 0.05$, $b = 1.7$ and $\alpha = 0.02$ K/m. In this case the parameter $s \gg 1$ so that $h(s) \approx 1$ (Eq. (16)) and Eq. (17) reduces to

$$\delta T(t) = \frac{2n\alpha v \rho_F c_F k_0}{\gamma b}\left(\frac{\beta_g t}{\pi \rho_g c_g}\right)^{1/2}. \quad (18)$$

Substituting the mentioned above parameters into Eq. (18) we find that $t \sim 6\times 10^6$ years. It should be noted that the typical period of mountain formation is of the order of 2.5×10^7 years, i.e., of the same order as t. This anomaly can be considered as stable since its duration is much longer than that used for observations and for obtaining the average values (few years).

A few comments are in order. First, we have to emphasize that the existence of high porosity up to the depth of the focal zone is not required for our mechanism. The formation of the system of coupled channels (percolation cluster) with porosity of 0.01–0.1 at depths up to 1–5 km, turns out to be sufficient to explain this effect. Then, besides of the interaction of different channels some of them can occasionally disappear and appear since the process itself has very long duration. In this consideration one may expect temporary enhancement in the rock permeability so that the average filtration velocity used above might be too small. Using the velocity $v = 10^{-5}$ m/s as an upper limit (Tronin, 1999), we obtain $t \sim 6\times 10^5$ years, that is one order of magnitude smaller than the above value.

We recall that Eq. (18) is valid under condition $t \ll L^2/D_g$. If this inequality is not satisfied then Eq. (A.19) should be used. Similar procedure of the temperature averaging leads to the estimate

$$\delta T = \frac{4nL\alpha v \rho_F c_F k_0}{\pi^2 \gamma b}. \quad (19)$$

Substituting $L = 10$ km and above parameters into Eq. (19) we obtain $\delta T \approx 0.3$ K, that is close to the observed value. Thus, the considered mechanism can explain, at least in principle, the existence of the stable thermal anomalies at the ground surface.

4. Discussion and conclusions

Our theoretical analysis has shown that stable ground temperature anomalies occasionally observed in seismo-active regions or in the vicinity of faults can be due to geothermal convective heat flow induced by slow filtration of the underground fluid. This heat flux is much smaller in magnitude than that arising from the solar radiation and other thermal fluxes of natural origin. Nevertheless this mechanism can play a substantial role in the presence of groundwater that can filtrate along the system of interconnected cracks in the upper crust. One can suppose that tectonic processes promote the increase in the crack concentration due to strong rock deformation and fracture near the faults. Thus, the rocks in the vicinity of this area differ from the surrounding media due to the presence of an enhanced porosity and permeability. The tectonic stress in the fault zone results in gradual squeezing-out of water from higher depth towards the ground surface. For this case the heating of the ground upper layers may arise due to upward fluid filtration from the bottom crust layers where the temperature is higher than in the upper layers. Our estimations show that this effect can really exist in spite of the smallness in the temperature difference between the upward moving fluid and surrounding rocks. The theory predicts a surface temperature increase or of a few K if the mean filtration velocity amounts to 10^{-6} m/s and if the mean rock porosity up to a depth of several kilometers exceeds the level of about $n = 0.01$–0.1. Moreover, this implies that the heating should last during the time interval which is smaller or the order of the typical duration of the mountain formation. Because of the long duration of the water squeezing-out process, the estimates obtained above hold regardless of the fact that in reality the filtration may occasionally slow down and then be reinforced due to the reconnection of underground channels that can occasionally appear/disappear.

Finally we arrive at the following conclusions:

1. Under certain conditions, existing in fault zone, the convection mechanism of the rock heating can result in the appearance of stable thermal anomalies in the surface ground temperature observed by the NOAA satellites above the seismo-active regions.
2. Our estimations show that appearance of anomalous regions with enhanced surface temperature of the order of a few K can arise on the geological time-scales.
3. The convection mechanism seems to have no effect during short time domain and thus cannot provide explanation of the non-stationary IR anomalies that occasionally appear several days before earthquakes. The latter might be due to other effects such as variation of the soil moisture, local greenhouse effect and etc.

Acknowledgements

This research was partially supported by the International Space Science Institute (ISSI) at Bern, Switzerland within the project "Earthquakes influence of the ionosphere as evident from satellite plasma density-electric field data", by the Commission of the EU (Grant No. INTAS-01-0456), by the Russian Fund for Basic Research through the Grant No. 04-05-64657 and by ISTC under Research Grant No. 2990. One of us (O.A.P.) wishes to thank the French Ministère de la Recherche et de la Technologie for hospitality at LPCE.

Appendix A

Here we present some necessary calculations that are used above in formulation of the model. Let us introduce a function U given by

$$U = T - T_a - \alpha z - \frac{q_r + q_{ev}}{\gamma}. \quad (A.1)$$

Then we substitute Eq. (A.1) into Eq. (10) and into the boundary conditions given by Eqs. (9), (11) and (12). Suppose that condition (11) is formally applied at $z = L$. Making a Fourier transform of Eqs. (9) and (10)–(12) we obtain

$$\mathrm{i}\omega u = D_g \nabla^2 u \quad (r > R,\ \ L > z > 0), \tag{A.2}$$

$$\partial_r u(R,z) = \frac{\mathrm{i}m}{\omega - \mathrm{i}\varepsilon}, \quad m = \frac{\alpha v \rho_F c_F R k_0}{2\beta_g}, \tag{A.3}$$

$$\partial_z u(r,0) = \frac{\gamma}{\beta_g} u(r,0), \tag{A.4}$$

$$\partial_z u(r,L) = 0. \tag{A.5}$$

Here u is the Fourier transform of the function U. To take correctly into account the residue of the function at $\omega = 0$, a small parameter ε is formally inserted in the denominator of Eq. (A.3). We shall substitute $\varepsilon = 0$ in the final expression.

Let us search for the solution of Eq. (A.2) in the form

$$u = \sum_{n=1}^{\infty} (A_n \sin \lambda_n z + B_n \cos \lambda_n z), \tag{A.6}$$

where A_n and B_n are constant values that should be found below.

Using Eq. (A.6) and the boundary conditions (A.4) and (A.5) one can find the connection of B_n with A_n

$$B_n = \frac{\beta_g \lambda_n}{\gamma} A_n, \tag{A.7}$$

and the equation which determines the eigenvalues λ_n

$$\lambda_n \tan \lambda_n L = \frac{\gamma}{\beta_g}. \tag{A.8}$$

The functions $f_n = \sin\lambda_n z + (\beta_g \lambda_n/\gamma)\cos\lambda_n z$ form a complete orthogonal system in the interval $0 \leqslant z \leqslant L$. Therefore, the boundary condition (A.3) can be expressed in a series of functions f_n

$$\partial_r u(R,z) = \frac{\mathrm{i}m}{\omega - \mathrm{i}\varepsilon} \sum_{n=1}^{\infty} C_n \left(\sin \lambda_n z + \frac{\beta_g \lambda_n}{\gamma} \cos \lambda_n z \right) \tag{A.9}$$

with

$$C_n = \frac{2}{\lambda_n L} \left[1 + \left(\frac{\beta_g \lambda_n}{\gamma} \right)^2 \right]^{-1} \left(1 + \frac{\beta_g}{\gamma L} \sin \lambda_n L \right)^{-1}. \tag{A.10}$$

Substitution of Eq. (A.6) with account of relation (A.7) into Eq. (A.2) leads to the Bessel equation for A_n

$$[d_r^2 + r^{-1} d_r - (\lambda_n^2 + \mathrm{i}\omega D_g^{-1})] A_n = 0, \tag{A.11}$$

where $d_r \equiv \mathrm{d}/\mathrm{d}r$ and $d_r^2 \equiv \mathrm{d}^2/(\mathrm{d}r)^2$.

The solution of Eq. (A.11), bounded at $r \to \infty$, is the modified Bessel function $K_0(\mu_n r)$ of the zero order with complex argument $\mu_n = (\lambda_n^2 + \mathrm{i}\omega D_g^{-1})^{1/2} (\mathrm{Re}\mu_n \geqslant 0)$.

Using boundary condition (A.9) from (A.11) we obtain

$$A_n = -\frac{\mathrm{i}m C_n K_0(\mu_n r)}{(\omega - \mathrm{i}\varepsilon)\mu_n K_1(\mu_n R)}, \tag{A.12}$$

where $K_1(x)$ is the modified Bessel function of the first order and coefficients C_n are defined by Eq. (A.10).

Eqs. (A.6)–(A.9) and (A.12) allows us to find u and after performing an inverse Fourier transform one can obtain U. Substituting this result into Eq. (A.1), the necessary temperature distribution is finally given by

$$T(r,z,t) = T_a + \alpha z + \frac{q_s(1-A) + q_{ev}}{\gamma} - \frac{\mathrm{i}m}{2\pi} \int_{-\infty}^{\infty} \frac{\exp(\mathrm{i}\omega t)\,\mathrm{d}\omega}{\omega - \mathrm{i}\varepsilon} \sum_{n=1}^{\infty} \frac{C_n K_0(\mu_n r)}{\mu_n K_1(\mu_n R)} \times \left(\sin \lambda_n z + \frac{\beta_g \lambda_n}{\gamma} \cos \lambda_n z \right). \tag{A.13}$$

The last term on the right in Eq. (A.13) describes the temperature increase caused by underground fluid. Let us average this value with respect to the square with radius $R_0 \gg R$. At the ground level $z = 0$ we get

$$\delta T(t) = \frac{2}{R_0^2} \int_0^{R_0} \delta T(r,0,t) r\,\mathrm{d}r = -\frac{\mathrm{i}m\beta_g}{\pi\gamma R_0^2} \int_{-\infty}^{\infty} \frac{\exp(\mathrm{i}\omega t)\,\mathrm{d}\omega}{\omega - \mathrm{i}\varepsilon} \times \sum_{n=1}^{\infty} \frac{\lambda_n C_n}{\mu_n K_1(\mu_n R)} \int_0^{R_0} K_0(\mu_n r) r\,\mathrm{d}r. \tag{A.14}$$

Since $R_0 \gg R$, we can set $R_0 \to \infty$ in the last integral in (A.14). Then after performing the integration over r we obtain

$$\delta T(t) = -\frac{\mathrm{i}\beta_g m R}{\pi R_0^2 \gamma} \sum_{n=1}^{\infty} \lambda_n C_n \int_{-\infty}^{\infty} \frac{\exp(\mathrm{i}\omega t)\,\mathrm{d}\omega}{(\omega - \mathrm{i}\varepsilon)(\lambda_n^2 + \mathrm{i}\omega D_g^{-1})}. \tag{A.15}$$

The integral (A.15) equals to the sum of residues of the integrand. Substituting $\varepsilon = 0$ in the final expression, we get

$$\delta T(t) = \frac{2\beta_g m R}{R_0^2 \gamma} \sum_{n=1}^{\infty} \frac{C_n}{\lambda_n} \left[1 - \exp(-\lambda_n^2 D_g t) \right]. \tag{A.16}$$

At $t \to \infty$ one can neglect the exponents in Eq. (A.16) and we arrive to exact solution of the problem for stationary case.

Now let us consider the specific case when $L \to \infty$, or more precisely $L \gg (D_g t)^{1/2}$. Then the solution of the characteristic Eq. (A.8) for λ_n reduces to $\lambda_n \to \pi(2n-1)/2L$, where n is integer, i.e., $n = 1, 2, 3, \ldots$ For large L values the shift $\delta\lambda_n = \pi/L \to 0$ and one can replace the summation over discrete n in Eq. (A.16) by corresponding integration over continuous variable λ. This gives

$$\delta T(t) = \frac{4\beta_g m R}{\pi R_0^2 \gamma} \int_0^{\infty} \frac{[1 - \exp(-\lambda^2 D_g t)]\,\mathrm{d}\lambda}{\lambda^2 (1 + \beta_g^2 \lambda^2/\gamma^2)}. \tag{A.17}$$

With the help of Eq. (A.3) expression (A.17) can be re-written as

$$\delta T(t) = \frac{2\alpha v R^2 \rho_F c_F L k_0}{\gamma R_0^2} \left(\frac{D_g t}{\pi} \right)^{1/2} \left(1 - \frac{\pi^{1/2}}{2 s^{1/2}} \left[1 - \exp(s) \mathrm{erfc}(s^{1/2}) \right] \right). \tag{A.18}$$

Here $\mathrm{erfc}(x) = 1 - \mathrm{erf}(x)$, $\mathrm{erf}(x)$ is the standard error function and $s = D_g t\gamma^2/\beta_g^2 = t\gamma^2/(c_g\rho_g)$.

In the opposite (quasi-stationary) case, $L \ll (D_g t)^{1/2}$, the expression (A.17) reduces to

$$\delta T = \frac{4\beta_g \gamma m R}{\pi R_0^2} \int_{\pi/(2L)}^{\infty} \frac{\mathrm{d}\lambda}{\lambda^2(\gamma^2 + \beta_g^2\lambda^2)} = \frac{4\alpha v R^2 \rho_F c_F k_0 L}{\pi^2 R_0^2 \gamma} \left[1 - \frac{\pi\beta_g}{2\gamma L}\left(\frac{\pi}{2} - \arctan\frac{\pi\beta_g}{2\gamma L}\right)\right]. \quad \text{(A.19)}$$

References

Abramowitz, M., Stegun, I.A., 1964. Handbook of Mathematical Functions, US Nat. Inst. of Standards and Technol., Gaithersburg, MD.

Babichev, A.P., Babushkina, N.A., Bratkovsky, A.M., et al., 1991. In: Grigorieva, I.S., Meilikhova, E.Z. (Eds.), Handbook of Physical Values. Energoatomizdat, Moscow (in Russian).

Barsukov, O.M., 1990. Estimate of magnetic perturbations of electrokinetic origin. Phys. Solid Earth 26, 125–128.

Carreno, E., Capote, R., Yaguy, A., et al., 2001. Observations of thermal anomaly associated to seismic activity from remote sensing, General Assembly of European Seismology Commission, Portugal, pp. 265–269.

Clark Jr., S.P., 1966. Thermal conductivity. In: Clark, S.P., Jr. (Ed.), Handbook of Physical Constants, Memoir 97. Geological Society of America, New York, pp. 459–482.

Clark Jr., S.P., 1969. Heat conductivity in the mantle. In: Hart, P.J. (Ed.), The Earth's Crust and Upper Mantle, Geophysical Monograph 13. American Geophysics Union, Washington, pp. 622–626.

De Groot, S.R., Mazur, P., 1962. In: Non-Equilibrium Thermodynamics. North-Holland, Amsterdam, pp. 405–452.

Gorny, V.I., Salman, A.G., Tronin, A.A., Shilin, B.B., 1988. The Earth outgoing IR radiation as an indicator of seismic activity. Proc. USSR Academy Sci. 301, 67–69.

Gorny, V.I., Shilin, B.B., Yasinsky, G.I., 1993. Thermal aerospace survey. Nedra, Moscow (in Russian).

Hayakawa, M., Molchanov, O., Tronin, A., Hobara, Y., Kodama, T., 2001. NASDA's earthquake remote sensing frontier research seismo-electromagnetic phenomena in the lithosphere, atmosphere and ionosphere, Final report, p. 229.

Liu, Qi-Qi, Ding, J., Cui, C., 2000. Probable satellite thermal infrared anomaly before the Zhangbei $M = 6.2$ earthquake on January 10, 1998. Acta Seimol. Sinica 13, 203–209.

Ma, Z., Gao, X., 1991. Application of space technique to earthquake hazards reduction in China, Preprint of Institute of Geology, Beijing, pp. 1–15 (in Chinese).

Mizutani, H., Ishido, T., Yokokura, T., Ohnishi, S., 1976. Electrokinetic phenomena associated with earthquakes. Geophys. Res. Lett. 3, 365–368.

Ouzounov, D., Freund, F., 2004. Mid-infrared emission prior to strong earthquakes analyzed by remote sensing data. Adv. Space Res. 33 (3), 268–273.

Pfannkuch, H.O., 1972. On the correlation of electrical conductivity properties of porous systems with viscous flow transport coefficients. In: Fundamentals of Transport Phenomena in Porous Media. Elsevier, New York, pp. 42–54.

Qiang, Z.J., Dian, C.G., 1992. Satellite thermal infrared impending temperature increase precursor of Gonghe earthquake of magnitude 7.0, Qinghai province. Geoscience 6, 297–300.

Qiang, Z.J., Xu, X.D., Dian, C.G., 1991. Thermal infrared anomaly—precursor of impending earthquakes. Chin. Sci. Bull. 36, 319–323.

Qiang, Z.J., Dian, C.G., Wang, X.J., Hu, S.Y., 1992. Satellite thermal infrared anomalous temperature increase and impending earthquake precursor. Chin. Sci. Bull. 37, 1642–1646.

Qiang, Z.J., Dian, C.G., Li, L.Z., 1999. Satellite thermal infrared precursor of two moderate-strong earthquakes in Japan and impeding earthquake prediction. In: Hayakawa, M. (Ed.), Atmospheric and Ionospheric Electromagnetic Phenomena Associated with Earthquakes. Terra Scientific Publishing Company, Tokyo, pp. 747–750.

Salman, A., Egan, W.G., Tronin, A.A., 1992. Infrared remote sensing of seismic disturbances. In: Polarization and Remote Sensing. SPIE, San Diego, CA, pp. 208–218.

Scholz, C.H., 1990. The Mechanics of Earthquakes and Faulting. Cambridge Univ. Press, Cambridge.

Tramutoli, V., Bello, D., Pergola, G.N., Piscitelli, S., 2001. Robust satellite technique for remote sensing of seismically active areas. Ann. Di Geofisica 44, 295–312.

Tronin, A.A., 1996. Satellite thermal survey—a new tool for the study of seismoactive regions. Int. J. Remote Sensing 17, 1439–1455.

Tronin, A.A., 1999. Satellite thermal survey application for earthquake prediction. In: Hayakawa, M. (Ed.), Atmospheric and Ionospheric Electromagnetic Phenomena Associated with Earthquakes. Terra Scientific Publishing Company, Tokyo, pp. 357–370.

Tronin, A.A., 2002. Atmosphere-lithosphere coupling. Thermal anomalies on the Earth surface in seismic processes. In: Hayakawa, M., Molchanov, O.A. (Eds.), Seismo Electromagnetics. Lithosphere–Atmosphere–Ionosphere Coupling. Terra Scientific Publishing Company, Tokyo, pp. 173–176.

Tronin, A.A., Hayakawa, M., Molchanov, O., 2002. Thermal IR satellite data application for earthquake research in Japan and China. J. Geodynam. 33, 519–534.

Veber, K., 1984. Remote sensing methods and catastrophes: the role of space images for prediction and reduction of losses due to geological catastrophes, 27 International Geological Congress, Moscow, 18, 1681–1687.

Wan, Z., Li, Z.-L., 1997. A Physics-based algorithm for retrieving land-surface emissivity and temperature from EOS/MODIS data. IEEE Trans. Geosci. Remote Sensing 35, 980–996.

Wang, L., Zhu, C., 1984. Anomalous variations of ground temperature before the Tangshan and Haiheng earthquakes. J. Seism. Res. 6, 649–656.